Correlations between azimuthal anisotropy Fourier harmonics in PbPb collisions at $\sqrt{s_{NN}} = 2.76$ TeV in the HYDJET++ model and in the multiphase transport model

M. Dordevic,[1] J. Milosevic,[1,2,*] L. Nadderd,[1] M. Stojanovic,[1] F. Wang,[3,4] and X. Zhu[3]

[1]*Vinca Institute of Nuclear Sciences, University of Belgrade, Vinca 11351, Belgrade, Serbia*

[2]*University of Oslo, Department of Physics, Blindern N-0316, Oslo, Norway*

[3]*College of Science, Huzhou University, Huzhou, Zhejiang 313000, P. R. China*

[4]*Department of Physics and Astronomy, Purdue University, West Lafayette 47907, Indiana, USA*

(Received 11 July 2019; published 10 January 2020)

Correlations between azimuthal anisotropy Fourier harmonics v_n ($n = 2, 3, 4$) are studied using the events from PbPb collisions at $\sqrt{s_{\rm NN}} = 2.76$ TeV generated by the HYDJET++ and multiphase transport (AMPT) models, and compared to the corresponding experimental results obtained by the ATLAS Collaboration. The Fourier harmonics v_n are measured over a wide centrality range using the two-particle azimuthal correlation method. The slopes of the v_2-v_3 correlation from both models are in a good agreement with the ATLAS data. The HYDJET++ model predicts a stronger slope for the v_2-v_4 and v_3-v_4 correlations than the ones experimentally measured, while the results from the AMPT model are in a rather good agreement with the experimental results. In contrast to the HYDJET++ predictions, the AMPT model predicts a boomeranglike shape in the structure of the correlations as found in the experimental data.

DOI: 10.1103/PhysRevC.101.014908

I. INTRODUCTION

Quantum chromodynamics predicts that at sufficiently high energy density partons can no longer be confined inside the nucleons. Indeed, a new state of matter with deconfined partons, called quark gluon plasma (QGP), is formed in ultrarelativistic nucleus-nucleus collisions [1,2]. The QGP undergoes a collective expansion, which can be described by relativistic hydrodynamics. The initial geometry of the colliding nuclei creates anisotropic pressure gradients in the transverse plane perpendicular to the beam direction. As a consequence, such initial spatial anisotropy is converted into momentum anisotropy observable in the final state as a preferential emission of particles in a certain azimuthal direction. The anisotropic flow can be studied by Fourier decomposition of the emitted hadron yield distribution in azimuthal angle ϕ [3–5]

$$\frac{dN}{d\phi} \propto 1 + 2\sum_n v_n \cos[n(\phi - \Phi_n)]. \tag{1}$$

Here, Fourier coefficient v_n represents the magnitude of the azimuthal anisotropy measured with respect to the nth-order harmonic plane angle Φ_n. The angle Φ_n can be reconstructed from the emitted particle distribution itself. The elliptic flow v_2 is the most studied anisotropy. The Φ_2, which corresponds to the v_2, is correlated with the participant plane spanned by the beam direction and the shorter axis of the roughly lenticular shape of the nuclear overlap region. The initial-state fluctuations in the positions of nucleons induce higher-order deformations, and thus higher-order Fourier harmonics [v_n, $n \geqslant 3$ in Eq. (1)] are present. Higher-order Fourier harmonics are measured with respect to the corresponding harmonic plane angles Φ_n [6]. The collective behavior of the QGP has been studied using the azimuthal anisotropy of emitted particles detected in experiments at the Relativistic Heavy Ion Collider (RHIC) [7–9] and the Large Hadron Collider (LHC) [10–21].

One of the experimental methods used to determine the v_n coefficients is based on two-particle azimuthal correlations [22]. These correlations can also be Fourier decomposed into

$$\frac{dN^{\rm pair}}{d\Delta\phi} \propto 1 + 2\sum_n V_{n\Delta} \cos(n\Delta\phi), \tag{2}$$

where $\Delta\phi$ is the relative azimuthal angle of the particle pair. Assuming the factorization, the two-particle Fourier coefficient $V_{n\Delta}$ is a product of the single-particle anisotropies of the particle pair. The v_n anisotropy can then be extracted by

$$v_n = \sqrt{V_{n\Delta}}, \tag{3}$$

with the two particles in the pair correlation belonging to the same particle group. For each event from a given centrality[1] class a two-dimensional two-particle correlation is constructed as a function of $\Delta\phi$ and relative pseudorapidity $\Delta\eta$. Typically, particles with $0.5 < p_T < 2$ GeV/c and $|\eta| < 2.5$ are used as we adopt in this study. In order to remove

*Corresponding author: Jovan.Milosevic@cern.ch

[1]The centrality of a nucleus-nucleus collision is defined as a fraction of the total inelastic nucleus-nucleus cross section, with 0% denoting the most central collisions.

short-range correlations only pairs with $|\Delta\eta| \geqslant 2$ are taken into account. One-dimensional correlation function in $\Delta\phi$ is built by projecting the two-dimensional correlation function onto the $\Delta\phi$ axis and then decomposed using Eq. (2).

This paper is organized as follows. The basic features of the HYDJET++ model [23] and the multiphase transport (AMPT) model [24] are described in Sec. II. Approximately 10^6 PbPb collision events at $\sqrt{s_{\rm NN}} = 2.76$ TeV each are simulated using the HYDJET++ (ver. 2.3) and AMPT (ver. 1.25-2.25) models. The results and discussions are given in Sec. III. The results are presented over a wide range of centralities going from ultracentral (0–5% centrality) to peripheral (65–70% centrality) PbPb collisions. A summary is given in Sec. IV.

II. HYDJET++ AND AMPT MODEL

The Monte Carlo HYDJET++ and AMPT models simulate relativistic nucleus-nucleus collisions. HYDJET++ consists of two components, which simulate soft and hard processes. The soft part governs the ideal hydrodynamical evolution of the system while the hard part provides multiparton fragmentation. The hard part of the HYDJET++ consists of PYTHIA [25] and PYQUEN [26] event generators, which simulate initial parton-parton collisions, radiative energy loss of partons, and parton hadronization. It also takes into account jet quenching effects within the formed medium. The minimum transverse momentum transfer $p_T^{\rm min}$ of a parton-parton scattering determines whether it contributes to the soft or the hard part. In the soft part of the HYDJET++ model, the elliptic flow magnitude is governed by the spatial anisotropy $\epsilon(b)$, which, at a given impact parameter b, represents the elliptic anisotropy of the hydrodynamics hypersurface at the freeze out, and by the momentum anisotropy $\delta(b)$, which is the modulation of flow velocity profile (see Eq. (34) in Ref. [23]). In the low-p_T range ($\leqslant$2 GeV/c), the elliptic flow is mainly determined by the internal pressure gradients developed within the expanding fireball during the initial phase of the collision, and is sensitive to the ϵ and δ parameters. As each fluid cell carries a certain momentum, at the freeze out the spatial anisotropy is transformed into the momentum anisotropy. In order to extend the HYDJET++ model to the triangular v_3 flow, additionally the third-order spatial $[\epsilon_3(b)]$ and momentum $[\rho(b)]$ anisotropy parameters are introduced. Simulation of the events can be performed under several configurations. The most realistic one, flow+quenched jets, which includes both hydrodynamics expansion and quenched jets, is used in this analysis. The details of the model can be found in the HYDJET++ manual [23].

A multiphase transport (AMPT) model [24] consists of several parts: the HIJING model [27], which generates semihard minijet partons and soft strings; string melting, which converts strings into partons; Zhang's parton cascade (ZPC) [28], which simulates the interactions among partons; the Lund string fragmentation [29,30] as implemented in JETSET/PYTHIA [31] to convert the excited strings into hadrons or a simple quark coalescence model to convert partons into hadrons in the case of string melting. Interactions among hadrons are described by the extended relativistic transport model. In this analysis, the default value of the parton cross section of 3 mb is used in ZPC. The running coupling α_s and the screen mass μ values of 0.4714 and 3.2264 fm^{-1} are used, respectively [32]. This, together with the assumed initial temperature of 468 MeV, gives an effective specific shear viscosity η/s of 0.137 based on Eq. (4) in Ref. [32]. Within the model, the anisotropies of different orders are developed due to the initial-state eccentricities. It was shown in Ref. [33] that in peripheral collisions the efficiency of converting the initial eccentricities into final momentum anisotropies decreases because of the reduced amount of interactions in the small system. More details about the AMPT model can be found in Ref. [24].

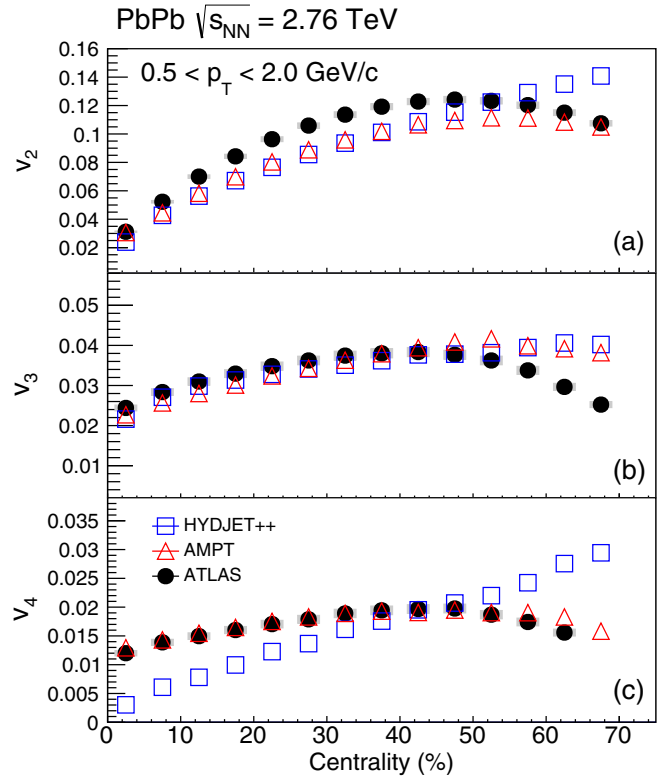

FIG. 1. The centrality dependence of the v_2 (top), v_3 (middle), and v_4 (bottom) from the $0.5 < p_T < 2$ GeV/c interval in PbPb collisions at 2.76 TeV [34]. The experimental data from ATLAS are shown by the closed circles. The results simulated by AMPT and HYDJET++ models are shown by the open red triangles and blue squares, respectively. The shadow boxes represent the systematic uncertainties of the experimental data, while the statistical uncertainties are smaller than the symbol size.

III. RESULTS

Centrality dependencies of the Fourier harmonics v_2, v_3, and v_4 from PbPb collisions at $\sqrt{s_{\rm NN}} = 2.76$ TeV simulated by the HYDJET++ and AMPT models are shown in Fig. 1 together with the experimental data from the ATLAS Collaboration [34]. In both models, the elliptic v_2 harmonic exhibits a strong centrality dependence, while the v_3 and v_4 have a weak centrality dependence. The v_2 in the HYDJET++

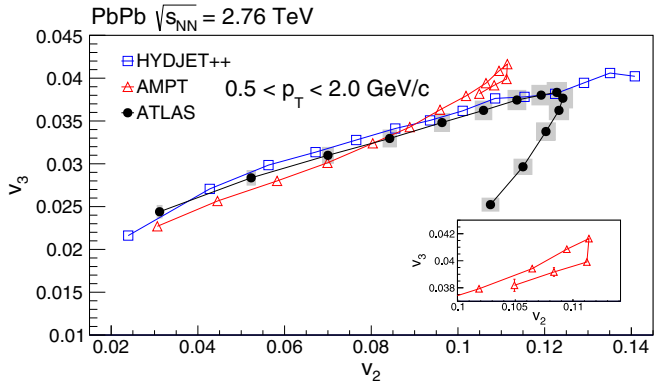

FIG. 2. The correlation between v_2 and v_3 from the $0.5 < p_T < 2$ GeV/c interval for fourteen 5%-wide centrality classes over the centrality range 0–70% in PbPb collisions at 2.76 TeV [34]. The results simulated by the AMPT and HYDJET++ models are shown by the open red triangles and blue squares, respectively. The shadow boxes represent the systematic uncertainties of the experimental data, while the statistical uncertainties are smaller than the symbol size.

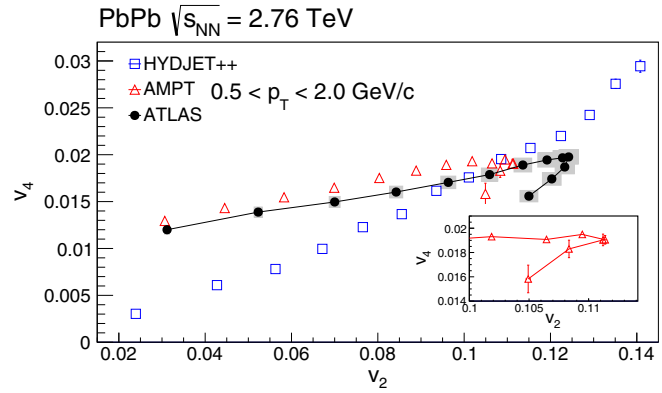

FIG. 3. The correlation between v_2 and v_4 from the $0.5 < p_T < 2$ GeV/c interval for 13 (14) 5%-wide centrality classes over the centrality ranges 0–65% (0–70%) in PbPb collisions at 2.76 TeV [34]. The results simulated by the AMPT and HYDJET++ models are shown by the open red triangles and blue squares, respectively. The error bars represent the statistical uncertainties. The shadow boxes represent the systematic uncertainties of the experimental data.

model continuously increases up to 70% centrality, while in the AMPT model it reaches its maximum at 50–60% centrality and than starts to decrease similarly to the experimental data. Except for the most central collisions where predictions from both models agree with the experimentally measured v_2, the models predict smaller elliptic flow than the data for centralities up to 50%. For centralities above 50%, the v_2 from the HYDJET++ model continues to increase and becomes greater than the experimental one. The v_3 extracted from both models is, up to 50% centrality, in a mutual agreement and in a good agreement with the experimentally measured v_3. For centralities above 50%, both models give v_3 greater than the experimentally measured one. The AMPT model prediction for v_4 Fourier harmonic is in a very good agreement with the experimentally measured v_4 for practically the whole centrality range, while the corresponding prediction from the HYDJET++ model disagrees with the experimental data. We note that the fourth-order spatial and momentum anisotropies are not implemented in the HYDJET++ model so the failure of the model in v_4 is expected. Based on these calculations, the correlations between Fourier harmonics of different orders are presented in the rest of the paper.

The correlation between the average v_2 and v_3 Fourier harmonics, where each point represents one centrality class, is shown in Fig. 2. In contrast to the v_2, higher-order Fourier harmonics v_n $(n = 3, 4)$ have a weak centrality dependence and in peripheral collisions they decrease faster than in central collisions as measured by ATLAS [34]. This introduces the appearance of a boomeranglike structure. The ideal hydrodynamics in the HYDJET++ model predicts nearly linear centrality dependence of the v_n harmonics, and thus does not produce the boomerang structure. The same behavior has been found in Ref. [35] with specific shear viscosity $\eta/s = 0$, while in the viscous hydrodynamics with positive η/s values, the v_n harmonics reach maxima and then decrease going to peripheral collisions. As a consequence, the boomeranglike shape appears in v_n-v_m correlations. The slopes of the v_2-v_3 dependence agree between the experimental data and the HYDJET++ model up to about 50% centrality. Going to more peripheral collisions, the difference starts to increase and show qualitatively different behavior. Up to 50% centrality, the magnitudes of the v_2 coefficients in the experimental data are greater than the ones predicted in the HYDJET++ model. For centralities above 50%, HYDJET++ predicts further increases of the v_2 and v_3 coefficients, while the experimental data show a decrease.

Unlike HYDJET++, the AMPT model predicts the slope as well as the boomeranglike shape of the correlation. However, the boomerang turn is much sharper than the one seen in the ATLAS data [34] (see the zoomed plot in Fig. 2). The experimental data from peripheral collisions shows a much faster decrease of the v_3 coefficient than the AMPT prediction where the decrease of the v_3 coefficient going to the peripheral collisions is the same as the decrease going to central collisions. For centralities above 35%, the v_3 coefficients from the AMPT model are greater than the ones measured by ATLAS, while for centralities below 20% the model results are somewhat smaller than the data. The relatively small partonic cross section used for this analysis of the AMPT model induces a significant effective specific shear viscosity [36], which produces maxima in the v_n distributions and then a decrease of the v_n going towards peripheral collisions.

Figure 3 shows centrality dependence of the correlation between v_2 and v_4 harmonics. Again, the experimental data [34] for very peripheral collisions show a boomerang shape, while the HYDJET++ model does not predict it. The HYDJET++ model predicts a much stronger slope than the one seen in the experimental data. Also, in central collisions, the HYDJET++ model predicts smaller v_4 values, while in peripheral collisions HYDJET++ gives greater v_4 values than the ones seen in the experimental data. Experimental v_2 values are greater than those extracted from the HYDJET++ simulation except for centralities above 50% where v_2 values continue to increase, while experimental ones start to

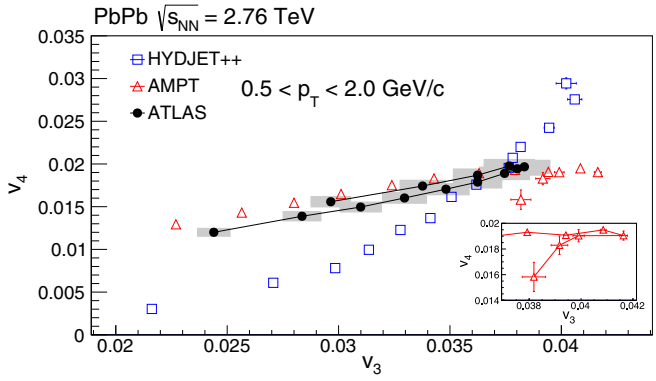

FIG. 4. The correlation between v_3 and v_4 from the $0.5 < p_T < 2$ GeV/c interval for 13 (14) 5%-wide centrality classes over the centrality range 0–65% (0–70%) in PbPb collisions at 2.76 TeV [34]. The results simulated by the AMPT and HYDJET++ are shown by the open red triangles and blue squares, respectively. The error bars represent the statistical uncertainties. The shadow boxes represent the systematic uncertainties of the experimental data.

decrease. In contrast to the v_3 anisotropy, the v_4 anisotropy is not introduced in the model via the corresponding eccentricity. Appearance of the higher-order harmonics v_n ($n > 3$) is a consequence of the interference of the v_2 and v_3 harmonics [37]. As there is a larger disagreement between HYDJET++ v_4 predictions and the data, this model does not describe the data well also in the v_2-v_4 correlation analysis.

Figure 3 also shows prediction of the AMPT model. The AMPT model reproduces the slope and the boomeranglike shape of the v_2-v_4 correlation (see the zoomed plot in Fig. 3). In contrast to the v_2-v_3 correlation, the AMPT model predicts the experimentally observed slope of the v_2-v_4 correlation even for peripheral collisions. The model reproduces rather well the experimentally measured v_4 values, while the v_2 values from AMPT are smaller than the measured ones except for the most central 0–5% collisions.

The correlation between v_3 and v_4 Fourier harmonics is shown in Fig. 4. Again, due to a larger disagreement between HYDJET++ v_4 predictions and the data, the HYDJET++ model predicts a steeper slope of v_3-v_4 correlation than the experimental data [34]. Similarly to the case of the v_2-v_4 correlation, the AMPT model reproduces the v_3-v_4 correlation observed in the experiment. For the peripheral collisions the AMPT model predicts the boomeranglike shape of the correlations with an opening angle similar to the one seen in the experimental data. However, it is worthwhile to note that there seems a subtle difference, namely, the data show a boomeranglike shape with a left turn, while the AMPT model predicts a right turn. Except for the most peripheral collisions, the AMPT model reproduces the magnitudes of the v_4 Fourier harmonic very well. For central collisions, the v_3 magnitudes are somewhat smaller than the experimentally measured ones, while for peripheral collisions the situation is opposite.

IV. SUMMARY

Centrality dependence of the correlations between v_2 and v_3, v_2 and v_4, and v_3 and v_4 are studied using two-particle correlation technique within $0.5 < p_T < 2.0$ GeV/c and $|\eta| < 2.5$ in PbPb collisions at $\sqrt{s_{NN}} = 2.76$ TeV simulated by the HYDJET++ and AMPT models. The results are compared to the corresponding experimental measurements obtained by the ATLAS Collaboration. In general, both models reproduce rather well the experimentally measured magnitudes of the Fourier harmonics v_n in central collisions. Going to more peripheral collisions, discrepancy between data and models becomes more pronounced. In the case of the correlations between v_2 and v_3, both the HYDJET++ and AMPT models reproduce rather well the slope. Because of a weak centrality dependence of the higher-order v_3 and v_4 Fourier harmonics, and a faster decrease of their magnitudes in peripheral rather than in central collisions, the experimental data exhibit a boomeranglike shape. This structure is not observed in the HYDJET++ model, but is reproduced by the AMPT model. Due to the disagreement between HYDJET++ v_4 predictions and the data, the HYDJET++ model does not reproduce the slopes in the correlations between v_2 and v_4 and between v_3 and v_4, while the AMPT model reproduces them well. In conclusion, the AMPT model reproduces the experimentally observed features of the correlations between Fourier harmonics of different orders better than the HYDJET++ model.

ACKNOWLEDGMENTS

The authors acknowledge the support of the Bilateral Cooperation between Republic of Serbia and People's Republic of China 451-03-478/2018-09/04 "Phenomenology in high energy physics". This work was supported in part by the Ministry of Education, Science and Technological Development of the Republic of Serbia (Grant No. 171019), the National Natural Science Foundation of China (Grant No. 11847315) and the US Department of Energy (Grant No. DE-SC0012910).

[1] E. V. Shuryak, Nucl. Phys. A **750**, 64 (2005).
[2] W. Busza, K. Rajagopal, and W. van der Schee, Ann. Rev. Nucl. Part. Sci. **68**, 339 (2018).
[3] J.-Y. Ollitrault, Phys. Rev. D **48**, 1132 (1993).
[4] S. Voloshin and Y. Zhang, Z. Phys. C **70**, 665 (1996).
[5] A. M. Poskanzer and S. A. Voloshin, Phys. Rev. C **58**, 1671 (1998).
[6] B. Alver and G. Roland, Phys. Rev. C **81**, 054905 (2010).
[7] B. B. Back *et al.* (PHOBOS Collaboration), Phys. Rev. Lett. **89**, 222301 (2002).
[8] K. H. Ackermann *et al.* (STAR Collaboration), Phys. Rev. Lett. **86**, 402 (2001).
[9] K. Adcox *et al.* (PHENIX Collaboration), Phys. Rev. Lett. **89**, 212301 (2002).
[10] K. Aamodt *et al.* (ALICE Collaboration), Phys. Rev. Lett. **105**, 252302 (2010).

[11] K. Aamodt *et al.* (ALICE Collaboration), Phys. Rev. Lett. **107**, 032301 (2011).
[12] B. B. Abelev *et al.* (ALICE Collaboration), J. High Energy Phys. 06 (2015) 190.
[13] J. Adam *et al.* (ALICE Collaboration), Phys. Rev. Lett. **116**, 132302 (2016).
[14] G. Aad *et al.* (ATLAS Collaboration), Phys. Lett. B **707**, 330 (2012).
[15] G. Aad *et al.* (ATLAS Collaboration), Phys. Rev. C **86**, 014907 (2012).
[16] G. Aad *et al.* (ATLAS Collaboration), J. High Energy Phys. 11 (2013) 183.
[17] S. Chatrchyan *et al.* (CMS Collaboration), Eur. Phys. J. C **72**, 2012 (2012).
[18] S. Chatrchyan *et al.* (CMS Collaboration), Phys. Rev. C **87**, 014902 (2013).
[19] S. Chatrchyan *et al.* (CMS Collaboration), Phys. Rev. C **89**, 044906 (2014).
[20] S. Chatrchyan *et al.* (CMS Collaboration), J. High Energy Phys. 02 (2014) 088.
[21] V. Khachatryan *et al.* (CMS Collaboration), Phys. Rev. C **92**, 034911 (2015).
[22] S. Wang *et al.*, Phys. Rev. C **44**, 1091 (1991).
[23] I. P. Lokhtin, L. V. Malinina, S. V. Petrushanko, A. M. Snigirev, I. Arsene, and K. Tywoniuk, Comput. Phys. Commun. **180**, 779 (2009).
[24] Z. W. Lin, C. M. Ko, B. A. Li, B. Zhang, and S. Pal, Phys. Rev. C **72**, 064901 (2005).
[25] T. Sjostrand, S. Mrenna, and P. Skands, J. High Energy Phys. 05 (2006) 026.
[26] I. P. Lokhtin and A. M. Snigirev, Eur. Phys. J. C **45**, 211 (2006).
[27] X. N. Wang and M. Gyulassy, Phys. Rev. D **44**, 3501 (1991).
[28] B. Zhang, Comput. Phys. Commun. **109**, 193 (1998).
[29] B. Andersson, G. Gustafson, G. Ingelman, and T. Sjöstrand, Phys. Rep. **97**, 31 (1983).
[30] B. Andersson, Camb. Monogr. Part. Phys. Nucl. Phys. Cosmol. **7**, 1 (1997).
[31] T. Sjöstrand, B. Soderberg, A Monte Carlo Program For Quark Jet Generation, LU TP 78-18.
[32] D. X. Wei, X. G. Huang, and L. Yan, Phys. Rev. C **98**, 044908 (2018).
[33] Y. Zhou, K. Xiao, Zh. Feng, F. Liu, and R. Snellings, Phys. Rev. C **93**, 034909 (2016).
[34] G. Aad *et al.* (ATLAS Collaboration), Phys. Rev. C **92**, 034903 (2015).
[35] J. Qian and U. Heinz, Phys. Rev. C **94**, 024910 (2016).
[36] Y. Zhou, Adv. High Energy Phys. **2016**, 9365637 (2016).
[37] L. V. Bravina, B. H. Brusheim Johansson, G. Kh. Eyyubova, V. L. Korotkikh, I. P. Lokhtin, L. V. Malinina, S. V. Petrushanko, A. M. Snigirev, and E. E. Zabrodin, Eur. Phys. J C **74**, 2807 (2014).